Idiopathic Growth Hormone Deficiency in the Morphologically Normal Pituitary Gland Is Associated with Perfusion Delay[1]

Chao-Ying Wang, BS
Hsiao-Wen Chung, PhD
Nai-Yu Cho, MS
Hua-Shan Liu, PhD
Ming-Chung Chou, PhD
Hung-Wen Kao, MD
Chun-Jung Juan, MD, PhD
Meei-Shyuan Lee, PhD
Guo-Shu Huang, MD
Cheng-Yu Chen, MD

Purpose: To investigate quantitatively the topographic perfusion characteristics of the adenohypophysis by using dynamic contrast material–enhanced magnetic resonance (MR) imaging in a subgroup of patients with idiopathic growth hormone deficiency (IGHD) and with normal-appearing pituitary morphology on MR images.

Materials and Methods: This HIPAA-compliant, prospective study was approved by an institutional review board, and informed consent was obtained for all patients. Twenty-five patients (mean age, 10.6 years ± 3.3 [standard deviation]) with clinical growth retardation, proved IGHD, and normal pituitary morphology on MR images were included for analysis. Sixteen children (mean age, 10.8 years ± 5.5) were included as control subjects. Time to peak (TTP) perfusion properties of the adenohypophysis in 10 regions of interest from multisection coronal dynamic contrast-enhanced T1-weighted MR images were quantitatively derived by using the Brix pharmacokinetic model. Significant difference was determined with a two-tailed Student *t* test. The Pearson correlation coefficient was used to correlate the perfusion parameters, including maximal enhancement peak and slope, with serum growth hormone levels in the IGHD group.

Results: TTP for the IGHD group was significantly prolonged compared with that for the control group ($P < .005$). The prolonged TTP in the IGHD group was found to be diffuse. The levels of growth hormone deficiency were negatively correlated with the peak enhancement and the slope of the wash-in phase, which suggests increased blood volume in IGHD within the pituitary gland.

Conclusion: IGHD and the degree of growth hormone deficiency are associated with nonregional perfusion delay in morphologically normal adenohypophyses. The lack of lateralization of perfusion delay may suggest that microvascular structural abnormalities play a role in IGHD.

[1] From the Department of Electrical Engineering, National Taiwan University, Taipei, Taiwan (C.Y.W., H.W.C., H.S.L., C.J.J.); Department of Radiology, Tri-Service General Hospital, 325 Cheng-Kung Road, NeiHu, Taipei, Taiwan 114, Republic of China (C.Y.W., H.W.C., N.Y.C., H.S.L., H.W.K., C.J.J., G.S.H., C.Y.C.); Institute of Biomedical Engineering, Yang-Ming University, Taipei, Taiwan (N.Y.C.); Department of Medical Imaging and Radiological Sciences, Kaohsiung Medical University, Kaohsiung, Taiwan (M.C.C.); and School of Public Health, National Defense Medical Center, Taipei, Taiwan (M.S.L.). From the 2003 RSNA Annual Meeting. Received March 18, 2010; revision requested May 4; revision received June 3; accepted June 22; final version accepted July 21. Supported in part by grant TSGH-C93-21, Medical Research Council under civil service of Tri-Service General Hospital. C.Y.C. supported in part by the National Science Council (grants NSC 98-2221-E-002-095-MY3 and NSC 97-2314-B-016-028-MY3). **Address correspondence to** C.Y.C. (e-mail: *sandy0928@seed.net.tw*).

Idiopathic growth hormone deficiency (IGHD) is the most common type among children with growth hormone deficiency. Although the pathogenesis of IGHD remains unclear, most investigators have suggested that perinatal injuries to the hypothalamic-pituitary axis, such as breech presentation and neonatal hypoglycemia, could be the possible causes (1,2). These hypotheses are likely based on the observations of morphologic alternations of the hypothalamus, pituitary stalk, and the pituitary gland in IGHD and in multiple pituitary hormone deficiency (3,4), in which typical magnetic resonance (MR) imaging findings often include a small pituitary gland and/or ectopic posterior lobe with or without a truncated stalk (5–7). However, morphologic changes in the pituitary gland may not be the sole determinant for inadequate secretion of growth hormone (8–10). Other underlying causes such as mutation of *GH1* or impaired perfusion may play a role (11,12).

Although the severity of IGHD can be assessed by using endocrinologic tests or conventional radiography for bone age, these tests do not reflect the underlying physiologic abnormality of the pituitary gland. Physiologic factors such as perfusion to the pituitary gland may be an important factor influencing hormone secretion (12–14). The complex hypophyseal-portal vasculature system consists of numerous small branches of indirect supplying vessels from the superior and inferior hypophyseal arteries and has a feature of interarterial anastomoses which may render adenohypophysis vulnerable to ischemia or pituitary apoplexy (15,16). Moreover, because the blood-brain barrier is absent in the pituitary gland, perfusion as measured with T1-weighted MR imaging with intravenous contrast medium is theoretically feasible. Recent advances in MR technique have made it possible to assess the pituitary gland at higher spatial and temporal resolution and speed than previously reported in the literature. Dynamic contrast material–enhanced T1-weighted MR imaging can help exploit tissue perfusion properties by using appropriate tracer kinetic models (17–19). Because the pituitary gland is a small, pea-shaped structure contained within a sellar fossa abutting the air-containing sphenoid sinus and clivus that is rich with marrow, the surrounding air and bone could cause susceptibility artifacts, making dynamic contrast-enhanced MR imaging study of the gland more difficult. Hence, early studies (12–14) using one section with 3- to 4-mm thickness on a sagittal plane had major limitations in the observation of the regional pituitary perfusion properties.

On the other hand, the topographic distribution of the somatotroph cells, a functional organization of pituitary cells, has been shown to be in the lateral portions of the anterior pituitary gland in an immunochemical study (20). It would be interesting to know if growth hormone deficiency is also topographically dependent in a similar way in terms of perfusion alterations. Therefore, the purpose of our study was to investigate quantitatively the topographic perfusion characteristics of the adenohypophysis by using dynamic contrast-enhanced MR imaging in a subgroup of patients with IGHD and with normal-appearing pituitary morphology on MR images.

Advances in Knowledge

- Characterization of topographic perfusion characteristics of the adenohypophysis by using dynamic contrast-enhanced MR imaging in patients with idiopathic growth hormone deficiency (IGHD) and with normal pituitary morphology is technically feasible.
- The time to peak (TTP) for the patients with IGHD was significantly prolonged compared with that for control subjects ($P < .005$).
- Prolonged TTP in the IGHD group was found to be diffuse.
- The levels of growth hormone deficiency were negatively correlated with the peak enhancement and slope of the wash-in phase, which suggests increased blood volume in the IGHD pituitary gland ($P < .05$).

Implications for Patient Care

- The knowledge that those with IGHD can have a normal-appearing adenohypophysis but abnormal pituitary perfusion may help radiologists better understand the limitations of morphologic MR imaging.
- Model-based dynamic contrast-enhanced MR imaging may help when growth hormone deficiency is suspected and when results of morphologic imaging of the pituitary gland are normal.

Materials and Methods

Subjects

The prospective study protocol was approved by the National Defense Medical Center and Tri-Service General Hospital institutional review board, and informed consent was obtained from all children's parents. This study was Health Insurance Portability and Accountability Act compliant. Between October 2002 and August 2009, 25 children with isolated IGHD (16 male patients, nine female patients; mean age, 10.6 years ± 3.3 [standard deviation]; age range, 6–17 years) were enrolled

Published online before print
10.1148/radiol.10100504

Radiology 2011; 258:213–221

Abbreviations:
IGHD = idiopathic growth hormone deficiency
ROI = region of interest
SNR = signal-to-noise ratio
TTP = time to peak

Author contributions:
Guarantors of integrity of entire study, C.Y.W., C.Y.C.; study concepts/study design or data acquisition or data analysis/interpretation, all authors; manuscript drafting or manuscript revision for important intellectual content, all authors; manuscript final version approval, all authors; literature research, C.Y.W., H.W.C., M.C.C., C.Y.C.; clinical studies, C.Y.W., H.W.C., N.Y.C., H.S.L., M.C.C., H.W.K., C.J.J., G.S.H., C.Y.C.; statistical analysis, C.Y.W., N.Y.C., M.S.L.; and manuscript editing, C.Y.W., H.W.C., H.S.L., G.S.H., C.Y.C.

Authors stated no financial relationship to disclose.

for dynamic contrast-enhanced MR imaging study. The inclusion criteria included *(a)* short stature, less than the third percentile or below 2 standard deviations of mean age-matched population height, *(b)* less than 2 years of skeleton maturation, *(c)* isolated growth hormone deficiency, less than 10 ng/mL peak serum growth hormone level with at least two provocative stimulations, and *(d)* normal pituitary glandular height, according to the reference values for those younger than 20 years from Argyropoulou et al (21). All children with IGHD were screened with a complete hypothalamic-pituitary function test to exclude the possibility of multiple pituitary hormone deficiency. In addition, children with stalk abnormality, including absence, thinning or transection, and/or ectopic posterior lobe of the pituitary gland, were excluded from the analysis. Five children were excluded according to the clinical criteria mentioned above. Three additional subjects were excluded because of poor image quality caused by motion artifacts. Altogether, eight patients were excluded, leaving 25 in the IGHD group for analysis. Another 16 children (eight male patients, eight female patients; mean age, 10.8 years ± 5.5; age range, 2–18 years), who had no clinical or laboratory evidence of pituitary dysfunction and were initially referred for MR study for reasons other than developmental delay such as headache, sinusitis, or orbital lesions, were included as the control group. The body heights and weights of the control group were within the normal ranges of the age-matched population. All control subjects had normal intracranial MR findings.

Table 1

Ten ROIs and Corresponding Abbreviations

Abbreviation	ROI
IS	Infundibulum stalk
AR	Right paramedian portion of the anterior section
AM	Middle portion of the anterior section
AL	Left paramedian portion of the anterior section
MR	Right paramedian portion of the middle section
MM	Middle portion of the middle section
ML	Left paramedian portion of the middle section
PR	Right paramedian portion of the posterior section
PM	Middle portion of the posterior section
PL	Left paramedian portion of the posterior section

Image Acquisition

MR studies were performed with a 1.5-T superconductive system (Magnetom Vision Plus; Siemens Medical System, Erlangen, Germany) by using a standard birdcage head coil. Patients first underwent standard axial fluid-attenuated inversion recovery and T2-weighted imaging and precontrast axial, coronal, and sagittal T1-weighted imaging. Dynamic contrast-enhanced imaging and subsequent postcontrast imaging were performed. Dynamic contrast-enhanced MR imaging was performed by employing a fast spin-echo technique with the following parameters: repetition time msec/echo time msec, 450/15; number of signals acquired, one; echo train length, seven; matrix size, 256 × 256; field of view, 140 × 140 mm; and section thickness, 2 mm. Three contiguous coronal sections without intersection gap were allocated on a midsagittal T1-weighted fast spin-echo image covering the anterior pituitary gland. Twelve serial dynamic images from each of the three coronal sections were acquired with an 18-second interval after manual bolus injection of 0.1 mmol gadopentetate dimeglumine (Magnevist; Bayer Schering, Berlin, Germany) per kilogram of body weight into the antecubital vein. The contrast medium injection was immediately followed by 20 mL of normal saline solution to flush the vein.

Data Analysis

Two neuroradiologists (C.Y.C. and H.W.K., with 20 and 5 years of experience, respectively), who were blinded to the subjects, evaluated the standard MR images of the IGHD and control groups at different sessions. Conventional images of the wrist for bone age assessment were also reviewed in the same way but only for the IGHD group. When there was a difference in reading results, a consensus was made to complete the rating. Each rater measured the heights of the pituitary glands according to the method proposed previously (21). Special attention was given to the midline sagittal T1-weighted sections for the assessment of the presence or absence of stalk abnormalities, the size of the anterior lobe, and the positions of the posterior lobe of the pituitary gland.

For dynamic contrast-enhanced MR imaging, a total of 36 images (three sections, 12 frames each) were transferred to a personal computer workstation and processed by using in-house software developed with Matlab (MathWorks, Natick, Mass). Ten regions of interest (ROIs) (Table 1) with uniform shape and size (16–20 pixels, 5.76–7.2 mm^2), including the infundibulum of the stalk and the central and bilateral paramedian portions of the anterior pituitary gland in three continuous sections (Fig 1), were chosen from the dynamic contrast-enhanced data sets by two experienced neuroradiologists (C.Y.C. and H.W.K.). To ensure reliability of the dynamic contrast-enhanced MR imaging data, quantitative analysis and error estimation were undertaken and are addressed in a later section. Quantitative perfusion parameters were analyzed separately on each ROI as follows: First, the signal intensity–time data were normalized and converted to relative concentration-time data (17,18). The concentration-time data (C_t) were then fitted, by using a nonlinear least-square curve fitting algorithm, to the Brix pharmacokinetic model as follows (19):

$$C_t = \frac{A}{k_{21} - K_{el}}\left(e^{-K_{el}\cdot t} - e^{-k_{21}\cdot t}\right),$$

Figure 1

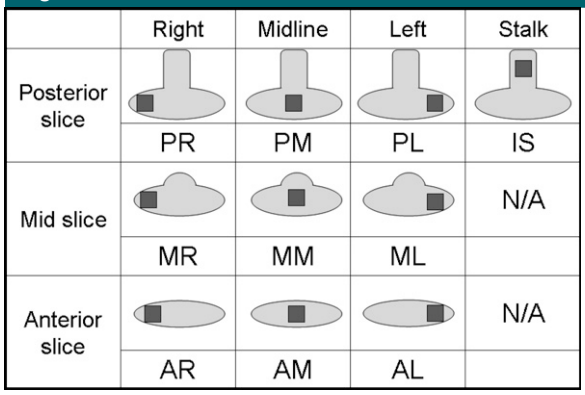

Figure 1: Schematic drawing of 10 ROIs selected for regional perfusion analysis from dynamic contrast-enhanced MR imaging acquisitions. *N/A* = not applicable.

where A is the amplitude scaling constant for the concentration-time curve of the plasma determined by factors such as the blood volume of the pituitary gland and so forth (17,18), K_{el} is the elimination transfer rate constant that describes the excretion of contrast agent through the kidneys, and k_{21} is the transfer rate constant describing the return of contrast agent from the extracellular extravascular space of the pituitary tissue to the plasma compartment. Goodness of fit was assessed by R^2 values as used in nonlinear curve fitting (22). After curve fitting, the analytic concentration-time data were used to obtain A, K_{el}, and k_{21}, followed by the derivation of three wash-in indexes: The peak enhancement (C_{max}) was defined as the maximal value of contrast agent concentration, the time to peak (TTP) (T_{max}) was defined as the time duration to reach C_{max}, and the slope of the wash-in phase was defined as C_{max}/T_{max}.

Error Assessment

Monte Carlo simulation at different levels of additive noise was used to estimate possible errors in the perfusion parameters derived from data sets acquired with finite temporal resolution and signal-to-noise ratio (SNR). A typical concentration-time curve obtained from one subject was taken first, along with the values of the perfusion parameters being recorded. An analytic concentration-time curve was generated from the perfusion parameters and treated as the noise-free reference curve. The reference curve was then sampled at an interval of 18 seconds to simulate the image acquisition procedure. Gaussian white noise was subsequently added to the concentration-time data at 10 SNR levels ranging from 5 to 50, with each SNR level containing 1000 sets of random noise. Nonlinear least-square error fitting to the Brix model was again performed on these simulated data to derive the three perfusion parameters (A, k_{21}, K_{el}) and was compared with the original values, with errors expressed as percentage deviation from the true values. Similarly, the percentage errors in peak enhancement, TTP, and slope of the wash-in phase were assessed.

Statistical Analysis

Sex and age distributions were examined by using the χ^2 test. The Student t test was used to examine the significant difference in perfusion parameters between the control and isolated IGHD groups. Correlation of the perfusion parameters with the growth hormone deficiency levels was made for the IGHD group by using the Pearson correlation coefficient. A P value less than .05 was considered to indicate a statistically significant difference.

Results

The demographic data of the IGHD group, including sex, age, bone age, body height and weight, and growth hormone level, are listed in Table 2. There was no significant difference in the distribution of age (P = .17) and sex ($P > .99$) between the control and IGHD groups. The mean heights of the pituitary glands in the control and IGHD groups were 6.0 mm ± 1.2 and 5.2 mm ± 0.9, respectively, which shows no significant difference ($P > .05$). In addition, the glandular heights were positively correlated with subject age (R^2 = 0.55) (Fig 2).

Fitting Error Assessment

Good curve fitting of the concentration-time data by using the nonlinear least-square algorithm (R^2 = 0.922 ± 0.049 in the control group and 0.966 ± 0.023 in the IGHD group) was obtained for our subjects. The residual errors in the signal enhancement of our data after nonlinear fitting were small (9.16% ± 4.82 and 6.32% ± 2.40 in the control and IGHD groups, respectively), which was consistent with the high R^2 values (Fig 3). Monte Carlo simulation showed that, at the SNR of 20, which was about the SNR level of all our dynamic contrast-enhanced data, the errors in A, k_{21}, and K_{el} were 33.5%, 30.1%, 32.8%, respectively. Because of high imprecision, these parameters were not used in subsequent comparisons. On the other hand, errors in C_{max}, TTP, and slope were 8.22%, 7.76%, and 14.7%, respectively, which shows better estimation reliability.

Regional Perfusion of Anterior Pituitary Gland between Groups

The 10 designated ROIs are illustrated on the coronal dynamic contrast-enhanced MR images shown in Figure 3a. Two representative concentration-time curves sampled from the posterior midline (or PM) ROIs of one IGHD and one control subject are shown in Figure 3b. Table 3 lists the perfusion parametric values derived from the 10 ROIs, as well as the statistical comparison results. Between-group comparison of the perfusion parameters with all ROIs averaged is shown in Figure 4. TTP and wash-in slope showed significantly higher and lower values, respectively, in the IGHD group than in the control group ($P < .0005$ for TTP, $P < .005$ for slope). Peak enhancement, on the other hand, showed no significant difference ($P > .05$) between the two groups. Regional analysis showed that TTP of the IGHD group was significantly delayed compared with that of the control group for all 10 ROIs ($P < .005$) (Fig 5).

Correlation of Growth Hormone Levels with Perfusion Parameters

The levels of growth hormone showed negative correlation with the wash-in slopes and peak enhancements of the entire anterior pituitary gland (r = −0.430, P = .036 and r = −0.493, P = .014, respectively) in the IGHD group (Fig 6). No significant correlation was found between the levels of growth hormone and TTP. When examining the individual ROIs, correlations existed only in the posterior right, posterior middle, posterior left, and middle right regions ($P < .05$).

Discussion

Our results were in concert with previous works in that the prolonged TTP enhancement and decreased wash-in slopes in the anterior pituitary lobe suggest insufficient perfusion, accompanied by a compensatory increase in blood volume, which is particularly true in those who had lower serum growth hormone level (Fig 6). The defected hypophyseal-portal system could compensate with higher perfusion efficiency, as we have observed significantly higher slope which was dominant in the posterior (posterior right, posterior middle, and posterior left) and the middle (middle right) sections of the anterior pituitary gland. The higher peak enhancement as seen in the posterior (right, middle, and left) and the middle (middle right) sections of anterior pituitary gland would suggest increased blood volume (a vasodilatory response) of the gland when cell apoptosis progresses.

Given the fact that most IGHD and multiple pituitary hormone deficiency cases commonly harbor structural abnormalities in the hypothalamic-pituitary axis, a subgroup of children with IGHD like our cases with normal morphology of the pituitary gland is considered uncommon, and the underlying pathogenesis becomes less consistent with those exhibiting a truncated stalk and a history of perinatal injury (23,24). From the diagnostic MR imaging perspective, functional rather than anatomic information may be needed to exploit this subgroup of patients when conventional

Table 2

Clinical Data of IGHD Group

Patient No./Sex/Age (y)	Bone Age (<2 years)*	Body Height (percentile)	Body Weight (percentile)	Growth Hormone Level (ng/mL)
1/F/13	11	<3rd	6th	3.2
2/M/12	8	<3rd	60th	5.7
3/F/11	9	<3rd	<3rd	8.6
4/F/11	8	15th	15th	7.1
5/M/13	11	<3rd	15th	5.3
6/F/13	11	3rd	>97th	1.4
7/M/5	2	<3rd	<3rd	3.9
8/F/6	4	<3rd	<3rd	6.7
9/M/7	4	4th	25th	9.6
10/M/11	8	8th	20th	9.1
11/M/6	4	10th	8th	8.6
12/M/12	5	<3rd	90th	0.1
13/M/8	5	<3rd	<50th	5.5
14/M/10	5	<3rd	75th	4.3
15/M/10	7	<3rd	13th	6.2
16/F/13	11	<3rd	<3rd	2.2
17/M/7	4	<3rd	<3rd	1.2
18/M/7	3	5th	10th	9.5
19/M/13	10	<3rd	20th	3.5
20/F/18	13	<3rd	<3rd	2.3
21/M/16	14	<3rd	9th	8.7
22/F/11	9	5th	50th	5.2
23/M/7	4	<3rd	4th	2.5
24/M/16	11	<3rd	<3rd	6.1
25/F/12	10	<3rd	<3rd	7.5

Note.—Average patient age was 10.6 years ± 3.3. Average serum growth hormone level was 5.36 ng/mL ± 2.8.

* Consists of less than 2 years of skeleton maturation.

Figure 2

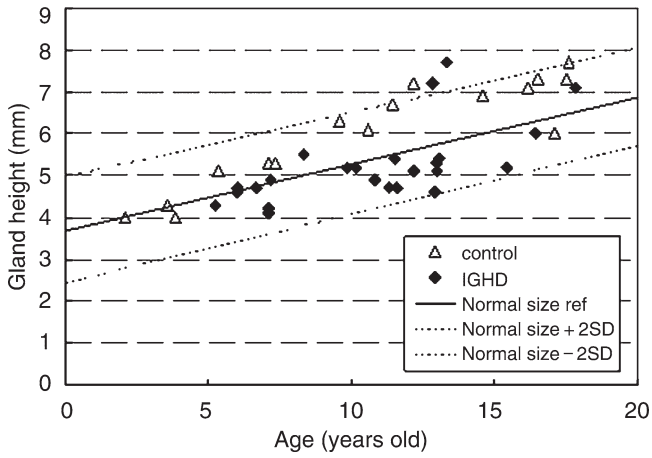

Figure 2: Graph shows distribution of anterior pituitary height for control (6.0 mm ± 1.2) and IGHD (5.2 mm ± 0.9) subjects, both with gland size falling within the normal range suggested in the literature as a function of age. Solid line = mean. Dotted lines = upper and lower bounds. Linear regression showed positive correlation of gland height with age (R^2 = 0.55), which was not significantly different compared with control subject data reported in the literature (P = .384).

Figure 3

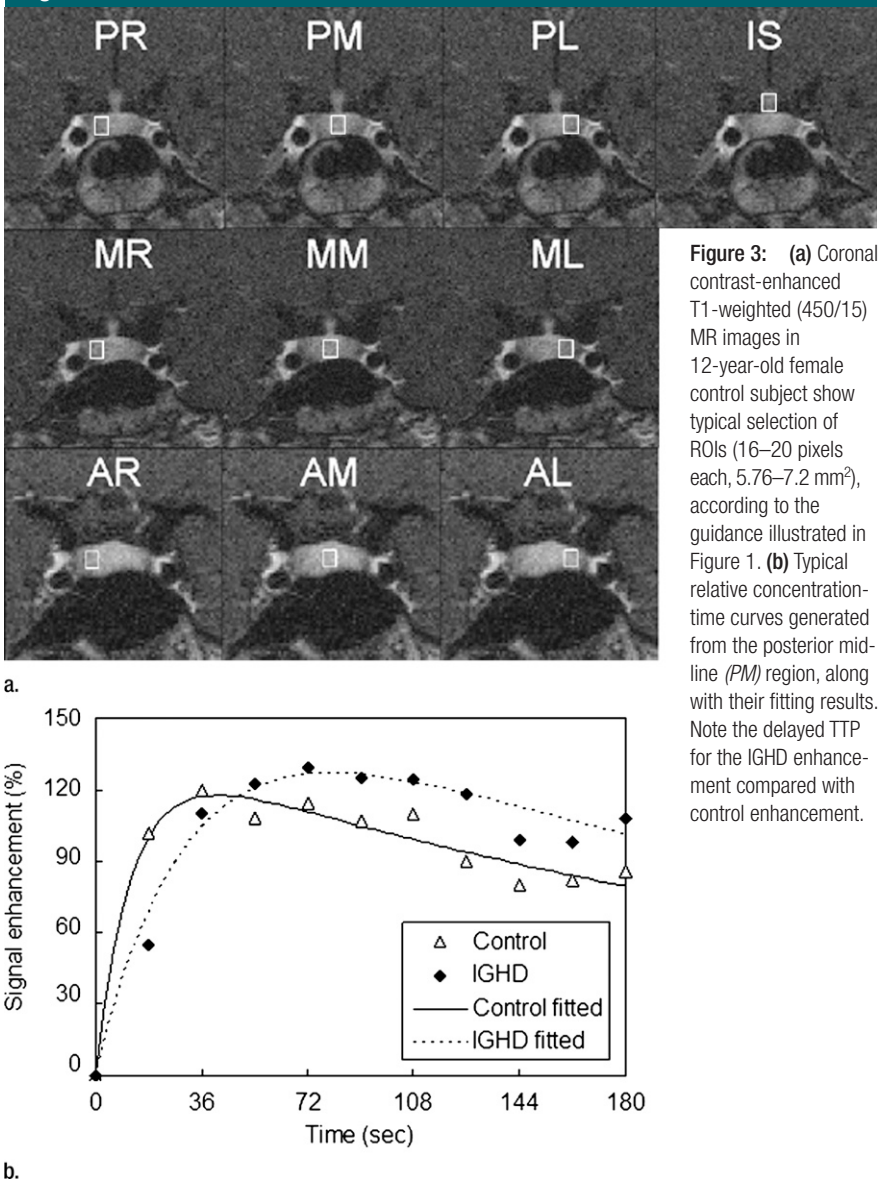

Figure 3: **(a)** Coronal contrast-enhanced T1-weighted (450/15) MR images in 12-year-old female control subject show typical selection of ROIs (16–20 pixels each, 5.76–7.2 mm^2), according to the guidance illustrated in Figure 1. **(b)** Typical relative concentration-time curves generated from the posterior midline *(PM)* region, along with their fitting results. Note the delayed TTP for the IGHD enhancement compared with control enhancement.

MR imaging results are normal. On the other hand, the growth responses of an individual patient to growth hormone treatment are variable. Growth hormone treatment may induce adverse events such as leukemia, benign intracranial hypertension, type II diabetes mellitus, and even death (25–27). A functional imaging tool for pituitary response monitoring may help to individualize patient treatments, especially in cases with progression from IGHD to multiple pituitary hormone deficiency.

Impaired blood perfusion to the anomalous hypothalamic-pituitary system in children with IGHD or multiple pituitary hormone deficiency has been implicated in two early studies with single-section dynamic contrast-enhanced MR imaging at low temporal and spatial resolution (12,14). Both studies showed delayed enhancement in growth hormone deficiency and multiple pituitary hormone deficiency groups, which suggests that abnormality of vasculature exists in hypophyseal arteries and the portal venous system. While it is understandable that delayed enhancement of the anterior pituitary lobe may occur in growth hormone deficiency or multiple pituitary hormone deficiency with stalk abnormalities because the main blood supply to the adenohypophysis is from the portal vasculature, it may be debatable when this occurs in patients with intact stalk morphology. In the Kornreich et al study (28), MR imaging findings of pituitary structural abnormality have contributed to the prediction of patterns and severity of hypopituitarism. It may appear that both types of IGHD (ie, types with and types without normal pituitary morphology) sustain the common feature of perfusion deficits, and the severity of perfusion impairments goes along with the levels of growth hormone deficiency as seen in our cases.

The functional cytomorphology of adenohypophysis with immunochemistry techniques is well documented (29). Growth hormone (somatotroph) cells account for approximately 50% of the pituitary cell mass and are anatomically distributed in the lateral and posterolateral portions of the adenohypophysis. Although the one-cell, one-hormone theory is no longer tenable, given that pluripotential cells are detected with more advanced techniques (30), somatotroph cells remain the main growth hormone secretary cells. The topographic lateralization of the somatotroph cells in adenohypophysis suggests that the diminished growth hormone secreting activity may be accompanied by decreased vascular perfusion in the capillary bed. To prove this point, a multiregional comparison of the perfusion properties in the entire anterior pituitary lobe with respect to that of a control is required. In our study, we conducted multisection and multiregional perfusion analysis for this purpose, and the results revealed region-independent perfusion delay in the IGHD group. This may explain in part that the pathogenesis of IGHD is multifactorial, and a single hormone deficiency could accompany global perfusion delay in the context of complicated vascular anatomy involved in the anterior pituitary gland. On the other hand, the findings of the overwhelming

Table 3

Regional Difference between IGHD and Control Group according to Perfusion Parameters

Perfusion Parameter	Region									
	PR	PM	PL	IS	MR	MM	ML	AR	AM	AL
Peak enhancement (%)*										
Control group	89.6 ± 43	89.2 ± 43	97.9 ± 35	77.3 ± 32	136.6 ± 33	143.9 ± 59	139.8 ± 27	129 ± 32	133.3 ± 49	124.2 ± 33
IGHD group	102.4 ± 51	90.6 ± 46	104.6 ± 48	72 ± 36	134.2 ± 51	130.9 ± 44	124.7 ± 45	114.9 ± 32	128.7 ± 50	117.6 ± 45
TTP (sec)†										
Control group	50.4 ± 12	31.2 ± 15	57.6 ± 18	28.3 ± 15	62.4 ± 21	39.6 ± 19	64.8 ± 17	65.6 ± 19	48.9 ± 18	64.3 ± 18
IGHD group	95.8 ± 27	62.6 ± 17	100.8 ± 29	45 ± 21	96.5 ± 26	68.4 ± 20	102.2 ± 34	111.1 ± 44	86.9 ± 34	121.3 ± 43
Slope (percentage per second)†										
Control group	1.8 ± 1	2.9 ± 1	1.7 ± 0	3.1 ± 1	2.4 ± 1	4.2 ± 2	2.4 ± 1	2.2 ± 1	3.2 ± 2	2.1 ± 1
IGHD group	1.1 ± 1	1.6 ± 1	1.1 ± 1	1.8 ± 1	1.5 ± 1	2.1 ± 1	1.4 ± 1	1.3 ± 1	1.7 ± 1	1.1 ± 1

Note.—Data are means ± standard deviations.

* *P* value for all ROIs was .05.

† *P* value for all ROIs was .005.

Figure 4

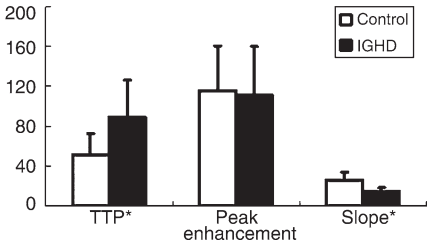

Figure 4: Graph shows comparison of TTP, peak enhancement, and wash-in slope of the entire anterior gland between the control and IGHD groups. The units of measure for the vertical axis are percentage per second for slope, percentage for peak enhancement, and second for TTP. Error bars = standard deviations. ∗ = significant difference. Data show delayed TTP and reduced wash-in slope in IGHD group at *P* less than .0005 and *P* less than .005 levels, respectively.

Figure 5

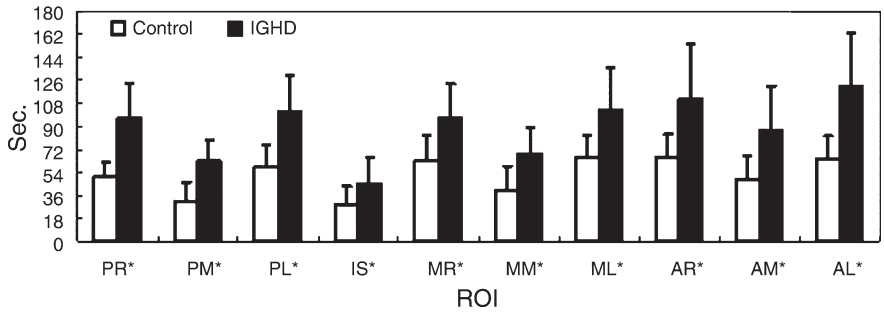

Figure 5: Graph of regional analysis of the TTP shows that IGHD group exhibits TTP values 1.5 to two times greater than that of the control group in all 10 ROIs ($P < .005$). In addition, the median parts (PM, IS, MM, and AM) of the anterior hypophysis showed faster wash-in than the bilateral parts (PR, PL, MR, ML, AR, and AL) in both groups ($P < .005$). ∗ = significant difference.

incidence of congenital anomalies in children with IGHD from the study by Garel and Léger (31) suggest that unenhanced MR imaging is appropriate for regular morphologic diagnosis. Our study further implied that, in a subgroup of children with IGHD and with normal pituitary morphology, dynamic contrast-enhanced MR imaging may help to delineate the intrinsic deficits such as delayed perfusion and increased blood volume in the adenohypophysis.

Although previous studies have shown similar delayed wash-in for the blood supply to the hypophyseal-portal system in dwarfism (12,14,32,33), several technical features used in our study provided key improvements toward successful quantification of the pituitary perfusion. Fast spin-echo acquisition was used instead of rapid gradient-echo acquisition (34,35) for dynamic imaging; thus, the possible susceptibility-induced signal loss from the air-tissue interface was alleviated. An appropriate pharmacokinetic model was used for curve fitting, with validating simulation performed; thus, the identification of peak enhancement was relatively immune to noise effects (36). With successful curve fitting, data analysis can be performed on a case-by-case basis as in routine diagnosis, as opposed to the use of group average for the concentration-time curves (12). Furthermore, quantitative derivation of the perfusion parameters allowed an objective exploration of the phenomena rather than merely descriptive investigations (14). Missing any elements from above might risk substantial lowering of the measurement accuracy.

There were some limitations to our study. First, the case numbers were small because of the relatively uncommon clinical entity and strict inclusion criteria. This, however, can be partially compensated by rigorous data collection and analysis of the dynamic MR data sets. That is why we tested the reliability

Figure 6

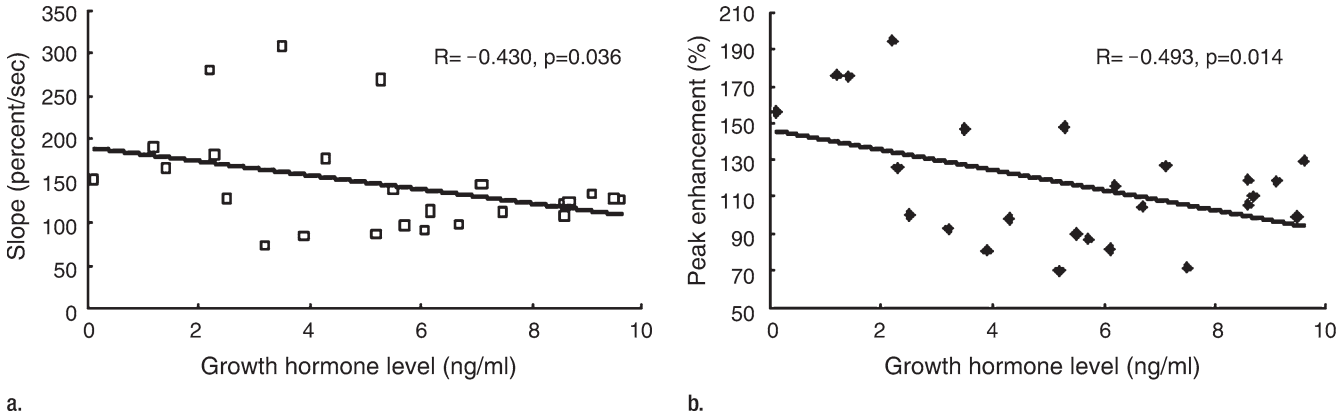

Figure 6: Graphs of growth hormone level in IGHD show negative correlation with **(a)** wash-in slope ($r = -0.430$, $P = .036$) and **(b)** peak enhancement ($r = -0.493$, $P = .014$) for the entire anterior pituitary. No correlation was found between the growth hormone level and TTP. When investigating individual ROIs, similar correlations existed only in PR, PM, PL, and MR regions ($P < .05$, data not shown). The results may suggest that the impaired perfusion in IGHD presented as delayed wash-in is accompanied by a compensating increase in blood volume, a vasodilatory response which was dominant in the posterior (PR, PM, and PL) and middle (MR) sections of the anterior pituitary gland.

and SNR dependency of the perfusion parameter calculations. Simulation results indicated that the estimation of the washout parameter K_{el} was prone to large errors, which originated from inadequate temporal coverage of our dynamic contrast-enhanced MR imaging protocol spanning less than 4 minutes. Accompanying the K_{el} imprecision were the consequently large errors in A and k_{21}. As a result, we restricted our data analysis within the wash-in phase for an accurate derivation of TTP, C_{max}, and the wash-in slope. Second, the temporal and spatial resolution of the dynamic contrast-enhanced MR images were still limited, though having been much improved compared with earlier studies, as far as the size of the anterior pituitary gland is concerned. Further technical improvements in dynamic MR imaging with shorter imaging time and higher temporal resolution, while maintaining a sufficient SNR level for reliable quantitative analysis, can help in this regard. Because we did not perform serial dynamic contrast-enhanced MR imaging studies individually over time, the longitudinal sensitivity of our perfusion quantification and its correlation to hormone level requires further investigation. Given that a reasonable SNR can be achieved and perfusion quantification can be done in small organs like the anterior pituitary gland, dynamic contrast-enhanced MR imaging may be potentially feasible to monitor the therapeutic response and to help in clinical decision making, especially for children with IGHD and normal morphology. Finally, although all control subjects had normal body heights, serum growth hormone levels and bone age information were not obtained because of the original experiment design that was partly compromised by the traditional Chinese folklore and ethical issue.

In conclusion, dynamic contrast-enhanced T1-weighted fast spin-echo MR imaging and Brix model analysis allow multisection and multiregional quantitative evaluation of the anterior pituitary gland in patients with IGHD and with normal pituitary morphology.

Acknowledgment: The authors thank Shih-I Tsao, BS, for MR data retrieving.

References

1. Craft WH, Underwoood LE, Van Wyk JJ. High incidence of perinatal insult in children with idiopathic hypopituitarism. J Pediatr 1980;96(3 pt 1):397–402.
2. Kucharczyk W. Etiology of congenital growth hormone deficiency. AJNR Am J Neuroradiol 2000;21(6):999–1000.
3. Kikuchi K, Fujisawa I, Momoi T, et al. Hypothalamic-pituitary function in growth hormone-deficient patients with pituitary stalk transection. J Clin Endocrinol Metab 1988;67(4):817–823.
4. Murray PG, Hague C, Fafoula O, et al. Likelihood of persistent GH deficiency into late adolescence: relationship to the presence of an ectopic or normally sited posterior pituitary gland. Clin Endocrinol (Oxf) 2009;71(2):215–219.
5. Kelly WM, Kucharczyk W, Kucharczyk J, et al. Posterior pituitary ectopia: an MR feature of pituitary dwarfism. AJNR Am J Neuroradiol 1988;9(3):453–460.
6. Root AW, Martinez CR, Muroff LR. Subhypothalamic high-intensity signals identified by magnetic resonance imaging in children with idiopathic anterior hypopituitarism: evidence suggestive of an 'ectopic' posterior pituitary gland. Am J Dis Child 1989; 143(3):366–367.
7. Fujisawa I, Kikuchi K, Nishimura K, et al. Transection of the pituitary stalk: development of an ectopic posterior lobe assessed with MR imaging. Radiology 1987;165(2):487–489.
8. Zucchini S, di Natale B, Ambrosetto P, De Angelis R, Cacciari E, Chiumello G. Role of magnetic resonance imaging in hypothalamic-pituitary disorders. Horm Res 1995; 44(suppl 3):8–14.
9. Bozzola M, Adamsbaum C, Biscaldi I, et al. Role of magnetic resonance imaging in the diagnosis and prognosis of growth hormone deficiency. Clin Endocrinol (Oxf) 1996;45(1): 21–26.
10. Inoue Y, Nemoto Y, Fujita K, et al. Pituitary dwarfism: CT evaluation of the pituitary gland. Radiology 1986;159(1):171–173.

11. Binder G, Nagel BH, Ranke MB, Mullis PE. Isolated GH deficiency (IGHD) type II: imaging of the pituitary gland by magnetic resonance reveals characteristic differences in comparison with severe IGHD of unknown origin. Eur J Endocrinol 2002;147(6):755–760.
12. Liu HM, Li YW, Tsai WY, Su CT. Dynamic enhancement MRI of anterior lobe in pituitary dwarfism. Neuroradiology 1995;37(6): 486–490.
13. Tien RD. Sequence of enhancement of various portions of the pituitary gland on gadolinium-enhanced MR images: correlation with regional blood supply. AJR Am J Roentgenol 1992;158(3):651–654.
14. Maghnie M, Genovese E, Aricò M, et al. Evolving pituitary hormone deficiency is associated with pituitary vasculopathy: dynamic MR study in children with hypopituitarism, diabetes insipidus, and Langerhans cell histiocytosis. Radiology 1994;193(2):493–499.
15. Sheehan HL, Stanfield JP. The pathogenesis of post-partum necrosis of the anterior lobe of the pituitary gland. Acta Endocrinol (Copenh) 1961;37(4):479–510.
16. Reid RL, Quigley ME, Yen SS. Pituitary apoplexy: a review. Arch Neurol 1985;42(7): 712–719.
17. Buckley DL, Kerslake RW, Blackband SJ, Horsman A. Quantitative analysis of multislice Gd-DTPA enhanced dynamic MR images using an automated simplex minimization procedure. Magn Reson Med 1994;32(5): 646–651.
18. Larsson HB, Stubgaard M, Frederiksen JL, Jensen M, Henriksen O, Paulson OB. Quantitation of blood-brain barrier defect by magnetic resonance imaging and gadolinium-DTPA in patients with multiple sclerosis and brain tumors. Magn Reson Med 1990; 16(1):117–131.
19. Brix G, Semmler W, Port R, Schad LR, Layer G, Lorenz WJ. Pharmacokinetic parameters in CNS Gd-DTPA enhanced MR imaging. J Comput Assist Tomogr 1991;15(4):621–628.
20. Elster AD. Modern imaging of the pituitary. Radiology 1993;187(1):1–14.
21. Argyropoulou M, Perignon F, Brunelle F, Brauner R, Rappaport R. Height of normal pituitary gland as a function of age evaluated by magnetic resonance imaging in children. Pediatr Radiol 1991;21(4):247–249.
22. Bates D, Watts D. Nonlinear regression: iterative estimation and linear approximations. In: Nonlinear regression analysis and its applications. New York, NY: Wiley, 1988;33–66.
23. Kuroiwa T, Okabe Y, Hasuo K, Yasumori K, Mizushima A, Masuda K. MR imaging of pituitary dwarfism. AJNR Am J Neuroradiol 1991;12(1):161–164.
24. Tillmann V, Tang VW, Price DA, Hughes DG, Wright NB, Clayton PE. Magnetic resonance imaging of the hypothalamic-pituitary axis in the diagnosis of growth hormone deficiency. J Pediatr Endocrinol Metab 2000; 13(9):1577–1583.
25. Blethen SL, Allen DB, Graves D, August G, Moshang T, Rosenfeld R. Safety of recombinant deoxyribonucleic acid-derived growth hormone: The National Cooperative Growth Study experience. J Clin Endocrinol Metab 1996;81(5):1704–1710.
26. Taback SP, Dean HJ. Mortality in Canadian children with growth hormone (GH) deficiency receiving GH therapy 1967-1992. The Canadian Growth Hormone Advisory Committee. J Clin Endocrinol Metab 1996; 81(5):1693–1696.
27. Nishi Y, Tanaka T, Takano K, et al. Recent status in the occurrence of leukemia in growth hormone-treated patients in Japan: GH Treatment Study Committee of the Foundation for Growth Science, Japan. J Clin Endocrinol Metab 1999;84(6):1961–1965.
28. Kornreich L, Horev G, Lazar L, Schwarz M, Sulkes J, Pertzelan A. MR findings in growth hormone deficiency: correlation with severity of hypopituitarism. AJNR Am J Neuroradiol 1998;19(8):1495–1499.
29. Horvath E, Kovacs K. Fine structural cytology of the adenohypophysis in rat and man. J Electron Microsc Tech 1988;8(4):401–432.
30. Scheithauer BW, Horvath E, Kovacs K, Laws ER Jr, Randall RV, Ryan N. Plurihormonal pituitary adenomas. Semin Diagn Pathol 1986; 3(1):69–82.
31. Garel C, Léger J. Contribution of magnetic resonance imaging in non-tumoral hypopituitarism in children. Horm Res 2007;67(4): 194–202.
32. Sato N, Sze G, Endo K. Hypophysitis: endocrinologic and dynamic MR findings. AJNR Am J Neuroradiol 1998;19(3):439–444.
33. Manfré L, Midiri M, Rosato F, Janni A, Lagalla R. Perfusion MRI in normal and abnormal pituitary gland: a preliminary study. Clin Imaging 1997;21(5):311–318.
34. Sakamoto Y, Takahashi M, Korogi Y, Bussaka H, Ushio Y. Normal and abnormal pituitary glands: gadopentetate dimeglumine-enhanced MR imaging. Radiology 1991;178(2): 441–445.
35. Stadnik T, Stevenaert A, Beckers A, Luypaert R, Buisseret T, Osteaux M. Pituitary microadenomas: diagnosis with two- and three-dimensional MR imaging at 1.5 T before and after injection of gadolinium. Radiology 1990; 176(2):419–428.
36. Maier C, Riedl M, Clodi M, et al. Dynamic contrast-enhanced MR imaging of the stimulated pituitary gland. Neuroimage 2004; 22(1):347–352.